Density Isobar of Water and Melting Temperature of Ice: Assessing Common Density Functionals

Pablo Montero de Hijes[1,2,*], Christoph Dellago[1], Ryosuke Jinnouchi[3], and Georg Kresse[1,4]
[1] *University of Vienna, Faculty of Physics, Kolingasse 14, A-1090 Vienna, Austria*
[2] *University of Vienna, Faculty of Earth Sciences,*
Geography and Astronomy, Josef-Holaubuek-Platz 2, 1090 Vienna, Austria
[3] *Toyota Central R&D Labs., Inc., 41-1 Yokomichi, Nagakute, Aichi 480-1192, Japan and*
[4] *VASP Software GmbH, Berggasse 21, A-1090 Vienna, Austria*

We investigate the density isobars of water and the melting temperature of ice using six different density functionals. Machine-learning potentials are employed to ensure computational affordability. Our findings reveal significant discrepancies between various base functionals. Notably, even the choice of damping can result in substantial differences. Overall, the outcomes obtained through density functional theory are not entirely satisfactory across most utilized functionals. All functionals exhibit significant deviations either in the melting temperature or equilibrium volume, with most of them even predicting an incorrect volume difference between ice and water. Our heuristic analysis indicates that a hybrid functional with 25% exact exchange and van der Waals damping averaged between zero and Becke-Johnson dampings yields the closest agreement with experimental data. This study underscores the necessity for further enhancements in the treatment of van der Waals interactions and, more broadly, density functional theory, to enable accurate quantitative predictions for molecular liquids.

[*] pablo.montero.de.hijes@univie.ac.at

Water is ubiquitous on our planet, and life on Earth is unthinkable without water. It is not surprising, therefore, that water has received a great deal of attention from the scientific community. It was also one of the first liquids to be intensively studied by computer simulations [1, 2]. Today, carefully constructed force fields play a key role in the study of water [3–29]. The best force fields are constructed to give an excellent description of all relevant properties of water (density, volume, isobars, phase transitions, etc.) while also giving outstanding agreement with high-level quantum chemistry calculations for small clusters. More recently, there has been a gradual shift toward supplementing or even substituting force fields with first-principles electronic structure calculations. These calculations predominantly rely on density functional theory (DFT), with the initial studies emerging in the early 1990s [30–33]. As computer power improved, the calculations moved towards relevant timescales and system sizes [34–47]. The advent of machine learning potentials has led to a further leap in the number of properties that can be predicted and the timescales that can be simulated [48–61]. Especially notable is the capability to simulate density isobars and melting temperatures within a matter of days or even hours, rendering the comparison of these properties with experimental data straightforward.

Surprisingly, or perhaps not so surprisingly, when using DFT, the agreement with experimental data is at best reasonable. Indeed, there is little doubt that the density isobars predicted by density functional theory are not yet on par with those obtained from carefully constructed semi-empirical models. So why bother with the costly density functional theory calculations? The explanation is straightforward: as our microscopic understanding of water has progressed over time, the scientific community has redirected its focus toward more intricate questions. These encompass the interactions between water and surfaces, the nucleation of water at nanoparticles, and processes like the electrolysis-induced hydrogen production or the hydrogen-to-water conversion in fuel cells. Understanding the interface between water and surfaces, frequently metallic ones, is imperative across these cases. Particularly, the simulations of electrolysis and fuel cells, where bonds are continuously broken and reformed, necessitate the application of first-principles calculations. However, conducting high-level quantum chemical calculations, for which some force fields have been calibrated, remains challenging for surfaces, or practically impossible for metallic ones. Consequently, density functional theory is the go-to approach. Nonetheless, employing density functional theory potentially adversely impacts the properties of water, as already discussed above. So ideally, one seeks a density functional that accurately describes the liquid state of water, encompassing at least the density and melting temperature. Thus, identifying a density functional that reasonably describes the properties of water is a pressing scientific issue that will strongly impact future water studies. Finding a suitable functional is the core goal of the present work.

Our methodology closely follows our previous work [62], where we have constructed machine-learning potentials (MLPs) for water for one semi-local density functional. The adopted strategy uses first on-the-fly training following the isobars using NPT simulations. Simulations cover ice, melting of ice and water in a temperature range between the supercooled state to slightly below the evaporation point. Further structures are added from parallel-tempering simulations along the isobar of water. The final dataset consists of about 1500 structures with typically 64 molecules. To obtain a highly accurate database, we have opted to use the hardest and most accurate potentials available for VASP[63, 64] (O_h and H_h). For the present work, we exclusively use the MLP implementation available in VASP. The on-the-fly training relies on Gaussian process regression using Bayesian regression [65–67]. However, for the production runs we rely on kernel-ridge regression[68, 69].

In a first attempt, we re-calculated the entire database using the desired functional. We expect this strategy to work well for functionals that yield a volume within 5% of the base functional (RPBE-D3), as the volume fluctuations during training are typically 5%. For SCAN (very different melting temperature and density) and optPBE (significantly larger density), we performed a complete on-the-fly training. For the hybrid functional revPBE0, we first upgraded a smaller on-the-fly RPBE-D3 database containing 662 structures to revPBE0-D3/zd using Δ-learning (database 2 in Ref. [62]), then continued training starting from this force field and refining it using on-the-fly training. This on-the-fly training was done using the hybrid functional, an energy cutoff of 1100 eV, and cooling liquid water twice from 350 K and 320 K, respectively, to 250 K, as well as melting cubic ice. The final dataset comprises 1010 structures.

To obtain the final MLPs for hybrid functionals, baseline RPBE-D3 calculations were conducted at 2000 eV. Subsequently, Δ-learning was employed to "upgrade" this dataset to different hybrid functionals. This was achieved by adding to the baseline database the energy, force and stress differences between the desired hybrid functional and the RPBE-D3 functional at 1100 eV. To reduce errors, all structures generated with the hybrid functional were used in the database for Δ-learning. However, in independent tests, we found that using 5 and 64 structures resulted in test set errors of 6 meV/Å and 2.5 meV/Å for the difference between two functionals. This does not add a significant error to the baseline error of about 26 meV/Å (error propagation follows the Gaussian law). So the Δ-learning approach taken here is on the safe side and does not introduce a noteworthy error. Indeed, comparison with a test set calculated at 2000 eV using the hybrid functional gives a force error of 28 meV/Å, which is only slightly larger than the errors we found for semi-local density functionals (26 meV/Å). The final database used for hybrid functionals covers a much larger set of volumes than the original database and we term it "hybrid".

Nevertheless, it is important to be cautious when employing Δ-learning. The primary sources of error stem not from capturing the difference between the two functionals, but rather from potential gaps in the training dataset, which may fail to cover the necessary range of configurations. Consequently, predictions for the *baseline semi-local* functional can become relatively inaccurate, in the present case, if there is a significant difference between the volumes predicted by the hybrid and semi-local functional. The hybrid dataset should remedy this issue, since it spans a volume range covering ±10% around the experimental density.

DFT	vdW	strategy
RPBE [70]	D3/zd [71]	base
RPBE	D3/BJ [72]	base
revPBE [73]	D3/zd	base
revPBE	D3/BJ	base
optPBE [74]		base & on-the-fly
SCAN [75]		on-the-fly
revPBE0 [76]	D3/zd	hybrid
revPBE0	D3/BJ	base & hybrid
PBE0	D3/BJ	hybrid
PBE0	D3/zd	hybrid

TABLE I. Training strategy for the various functionals used in the present work. "Base" corresponds to the original RPBE-D3 database. For "Base" the original database was recalculated using the desired functional and then used to train an MLP. References to functionals and D3 method with the respective damping functions are shown.

Figure 1 shows the density-temperature isobars obtained using a Langevin thermostat (friction coefficient 2 ps^{-1}) and parallel tempering for 128 molecules (for details we refer to Ref. [62]). In most of the parallel-tempering simulations, we see that images at low temperatures tend to stop exchanging with images at higher temperatures and freeze at the same time. Although the structure of ordered ice is not recovered, we find that the density around 210 K is always very close to the density of hexagonal ice reported in Tab. II. This can also be seen in Fig. 2 where we show the difference in density between ice and water along the isobar. Therefore, we believe that these structures are best categorized as precursors of low-density amorphous ice [81–83].

The first important observation is that none of the functionals gives a satisfactory density for liquid water, which should be around 1 $\mathrm{g/cm}^3$. Also, the experimental density difference between liquid water and ice is not well reproduced; experimentally, ice is about 90 % less dense than water. We start the discussion with the semi-local revised Perdew-Burke-Ernzerhof (RPBE [70] and revPBE [73]) functionals, all of which consistently give too low densities. The results also depend very much on the choice of damping, *i.e.* how the attractive van der Waals (vdW) terms are "damped" to zero as the constituents approach each other. The damping is necessary because the approximate semi-local DFT functionals already account for some of the interactions associated with correlation effects. Observing such a strong dependence on the choice of damping is very disturbing. In particular, only the zero damping (zd), *i.e.* the original functional form proposed by Grimme *et al.*,[71] yields a higher density for water than for ice, while the Becke-Johnson damping (BJ)[72] incorrectly predicts ice to be denser than water so that the slope of the melting line is likely to be inverted.

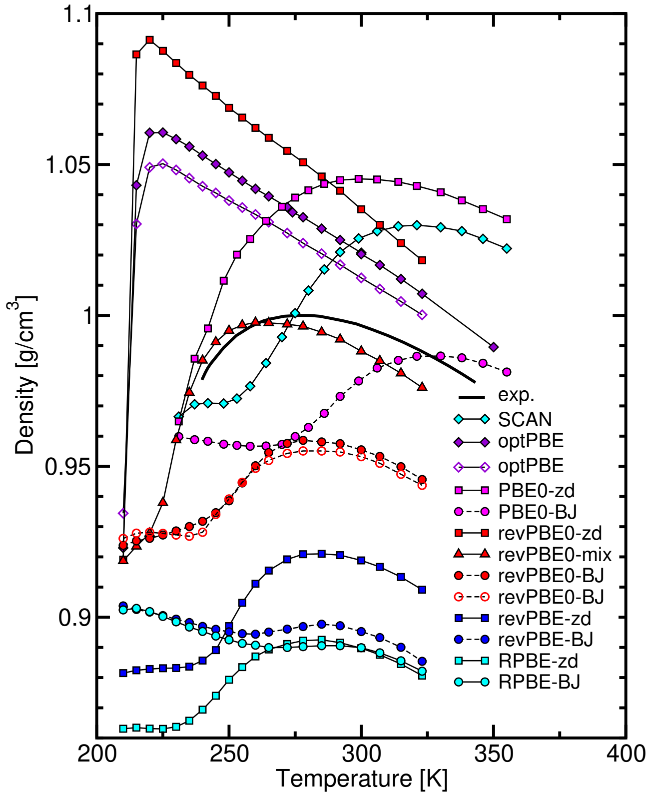

FIG. 1. Density as a function of temperature at a pressure of ∼ 1 bar (isobars). Results have been obtained using parallel-tempering simulations for 128 molecules, as detailed in Ref. [62]. Results for optPBE and revPBE0-D3/BJ shown using open symbols are obtained using the base dataset. The black solid line corresponds to experimental measurements (exp.) [77–80].

The baseline DFT functionals also have some influence on the results. The RPBE and revPBE functionals are closely related. The revPBE functional is a revised version of the original PBE functional. It includes modifications to the exchange part of the functional aimed at improving its accuracy in describing properties such as reaction energies of molecules. RPBE was primarily aimed at improving adsorption energies at surfaces and as opposed to revPBE locally observes the Lieb-Oxford criterion.[70] Overall, revPBED3-zd gives the best agreement with the experiment, although it underestimates the density of ice and, even more so, water. This underestimation is also true for the difference in densities between water and ice, as illustrated in Fig. 2. The ice melting points are presented in Table II. They were determined by performing anisotropic NpT calculations on 864 molecules at standard pressure and at various temperatures varying by 2 K. The temperatures reported are usually the average of the lowest temperature at which melting occurred and the highest temperature at which freezing occurred (or, in a few cases, the temperature at which neither freezing nor melting occurred). We expect the errors to be smaller than ±2 K, and note that agreement with our previously reported melting temperature for larger ensembles for RPBED3-zd is excellent. Table II shows that most semi-local functionals overestimate the experimental value of 273.15 K. Among these, the -zd ones align reasonably well, whereas the -BJ versions notably deviate, even exceeding the temperature of maximum density.

Now we discuss the results for hybrid functionals, as well as SCAN and optPBE. For optPBE and revPBE0-D3/BJ we illustrate results for the original database (open circles), as well as on-the-fly results for optPBE and results using the hybrid database covering a larger density variation for revPBE0-D3/BJ (filled circles). The predicted densities are somewhat too small using the databases constructed for RPBE-D3 structures, and the error increases as the density difference to RPBE-D3 increases. The error becomes even larger for revPBE0-D3/zd (not shown). This is a sign of the somewhat limited extrapolation capabilities of the MLPs applied in the present work, but we note that despite a density difference of 10-20% density errors remain below 1%.

Let us begin our more detailed discussion with optPBE, a functional that introduces vdW interactions through terms dependent on the density at two distinct points in space. This departs from conventional semi-local density functionals, which typically only consider semi-local information at a single point in space. As already noted above, the isobars for the two training sets are very similar. Both simulations lack a clear density maximum. Instead, the density increases almost linearly with decreasing temperature, with an abrupt jump to a low-density amorphous ice phase around 210 K. This result is reproducible, as confirmed by the two independent MLPs and thus independent of database details. A very similar unsatisfactory result is observed for revPBE0-D3/zd. Again, there is no discernible density maximum and an abrupt transition to a sort of low-density amorphous ice structure occurs around 210 K. Both functionals, optPBE and revPBE0-D3/zd, overestimate the density difference between water and ice, which appears to be the primary cause of the lack of a discernible density maximum. Also, their melting points occur at a very low temperature. On the other hand, the revPBE0-D3/BJ functional predicts densities that are too low, somewhat similar but slightly better than for the semi-local functionals with vdW corrections. Similar to revPBE0-D3/zd, PBE0-D3/zd yields a density that is too large but now a density maximum is discernible, albeit at a temperature that is too high, and the difference in density between water and ice is quite close to the experimental value. For PBE0-D3/BJ, the density isobar is very similar in shape to revPBE0-D3/BJ, but shifted to higher densities and temperatures. In fact, the melting points for all functionals are, in general, significantly too high, except for optPBE and revPBE0-D3/zd, which are too low.

It is worth noting that there are certain similarities between semi-local and hybrid functionals regarding the choice of the damping term. Specifically, the use of

Becke-Johnson (BJ) damping tends to increase the density of ice compared to water. While this adversely affects the performance of semi-local functionals, it has a somewhat positive effect on hybrid functionals, restoring the density maximum. But now the density difference between ice and water is again too small, so the agreement with the experiment is still far from good. Empirically mixing the machine-learning potentials for revPBE0-D3 with zero damping and revPBE0-D3 with Becke-Johnson damping yields the most favorable outcome (revPBE0-D3/mix). To do so, the energies, forces, and stress tensors in the two datasets are mixed using a weighting factor 1/2. This is equivalent to recalculating the entire database with a damping function between the two choices. This approach demonstrates excellent agreement in predicting the density difference between ice and water and results in a well-defined density maximum, albeit at temperatures that are somewhat lower than experimentally observed, and with the maximum in density occurring below the melting point. We estimate that a similar mixture for PBE0-D3 would also improve upon the standard dampings yielding a 1.5% too large density and an isobar maximum around 315 K.

Lastly, we comment on the results using the SCAN functional that are reasonable overall. We observe a difference in the water and ice density that closely matches the experimental difference but shifted to higher temperatures. Overall the density of water is about 5% too large, but that seems acceptable considering the larger errors of other functionals. The density maximum is, however, at a temperature (323 K) that is significantly too high, and the system freezes at far too low temperatures with respect to the temperature of maximum density, although still quite higher compared to experiments. So if one desires to simulate liquid water using SCAN, the temperature should be set well above 330 K.

In summary, we have assessed the density isobar of water and the melting temperature of ice for semi-local and hybrid functionals with vdW corrections across a range of commonly used density functionals. The outcomes, unfortunately, are not particularly pleasing, as none of the investigated functionals show good agreement with experimental density isobars. It is challenging to determine whether the inadequacy lies in the nature of the vdW correction or the specifics of the density functionals, but both factors likely contribute. Also, it is important to recognize that correlation effects are inherently non-separable, as they operate at all distances and wavelengths and electronic excitations at one length-scale mix with those at other length scales. This makes it challenging to isolate vdW interactions from other contributions. Employing a damping function to truncate vdW interactions at a certain range is necessarily heuristic, and even parameter fitting to an extensive dataset does not ensure accurate predictions beyond the test set or for very specific problems.

However, a few consistent observations emerge from our study: accurately reproducing the density difference between ice and water appears crucial for a reasonable isobar shape. Functionals that overestimate the density difference completely fail to generate a density maximum, instead leading to an abrupt transition to a low-density

DFT	vdW	ρ_{ice}	ρ_{water}	T_{m}	T_{max}
SCAN		0.966	1.025	299	321
optPBE		0.909	1.053	239	220
PBE0	D3-zd	0.960	1.045	303	300
PBE0	D3-BJ	0.951	0.987	330	327
revPBE0	D3-zd	0.905	1.073	246	220
revPBE0	D3-mix	0.910	0.997	270	263
revPBE0	D3-BJ	0.915	0.958	289	280
revPBE	D3-zd	0.875	0.921	283	284
revPBE	D3-BJ	0.895	0.890	314	287
RPBE	D3-zd	0.861	0.892	278	283
RPBE fly	D3-zd	0.861	0.892	278	283
RPBE	D3-BJ	0.892	0.887	310	289
Experimental		0.9999	1.0000	∼273	∼277

TABLE II. Density of hexagonal ice ρ_{ice} and water ρ_{water} at the melting temperature T_{m} for the functionals considered in the present work in g/cm. Values for the melting temperature T_{m} and the temperature of at the maximum density T_{max} are also shown in K.

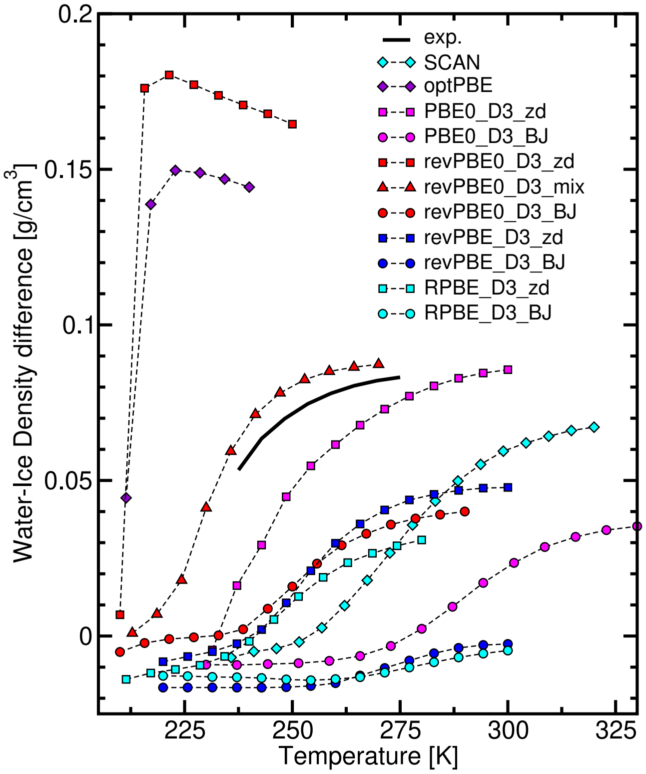

FIG. 2. Density difference between liquid water and ice as a function of temperature at a pressure of ∼ 1 bar (isobars). The solid black line shows the difference between the experimental value for liquid in Ref. [77] and for ice in Ref. [84].

amorphous ice phase (e.g. optPBE). Conversely, functionals with a small density difference or one in the correct range typically yield more reasonable isobar results, albeit potentially shifted in temperature and density. Notably, the SCAN functional falls into this latter category, with a density that is too high (5%) and a temperature deviation of almost 20%.

Among the semi-local functionals, we recommend either revPBE-D3/zd, as it provides the best overall density and accurate temperatures for the density maximum and melting, or RPBE-D3/zd, which is only slightly inferior for density, with a 4% larger error, although better in the melting point, both giving similar difference in density between water and ice. However, a common issue with all semi-local functionals based on revised versions of PBE is an underestimation of the density of ice and water. This might be partly caused by too long intramolecular O-H bonds (1 % too large for the revised PBE functions), but clearly this can be only part of the issue.

In the case of hybrid functionals, there are only marginal improvements. Results using zero damping are generally unsatisfactory, as the density difference between ice and water is too large, precluding the observation of an isobar density maximum resembling experimental results. Although BJ damping yields more reasonable results, they are not markedly superior to those using the semi-local functional RPBE-D3/zd. Empirically, we only achieve excellent agreement with the experiment when we combine an MLP with zero damping and BJ damping. We conclude that the state of density functionals for water is not satisfactory, and much more development effort will be required to resolve this issue.

This research was funded in part by the Austrian Science Fund (FWF) through the SFB TACO 10.55776/F81, and in part by 10.55776/I6467. For open access purposes, the author has applied a CC BY public copyright license to any author accepted manuscript version arising from this submission. Computer resources and technical assistance were provided by the Vienna Scientific Cluster (VSC). The authors have no conflicts to disclose. The datasets produced in this work are available upon reasonable request.

---

[1] J. Barker and R. Watts, "Structure of water; a monte carlo calculation," *Chemical Physics Letters*, vol. 3, no. 3, pp. 144–145, 1969.

[2] A. Rahman and F. H. Stillinger, "Molecular dynamics study of liquid water," *The Journal of Chemical Physics*, vol. 55, no. 7, pp. 3336–3359, 1971.

[3] V. Molinero and E. B. Moore, "Water modeled as an intermediate element between carbon and silicon," *The Journal of Physical Chemistry B*, vol. 113, no. 13, pp. 4008–4016, 2009.

[4] K. M. Dyer, J. S. Perkyns, G. Stell, and B. Montgomery Pettitt, "Site-renormalised molecular fluid theory: on the utility of a two-site model of water," *Molecular Physics*, vol. 107, no. 4-6, pp. 423–431, 2009.

[5] W. L. Jorgensen, "Quantum and statistical mechanical studies of liquids. 10. transferable intermolecular potential functions for water, alcohols, and ethers. application to liquid water," *Journal of the American Chemical Society*, vol. 103, no. 2, pp. 335–340, 1981.

[6] H. J. Berendsen, J. P. Postma, W. F. van Gunsteren, and J. Hermans, "Interaction models for water in relation to protein hydration," in *Intermolecular forces: proceedings of the fourteenth Jerusalem symposium on quantum chemistry and biochemistry held in jerusalem, israel, april 13–16, 1981*, pp. 331–342, Springer, 1981.

[7] W. L. Jorgensen, J. Chandrasekhar, J. D. Madura, R. W. Impey, and M. L. Klein, "Comparison of simple potential functions for simulating liquid water," *The Journal of Chemical Physics*, vol. 79, no. 2, pp. 926–935, 1983.

[8] H. J. Berendsen, J. R. Grigera, and T. P. Straatsma, "The missing term in effective pair potentials," *Journal of Physical Chemistry*, vol. 91, no. 24, pp. 6269–6271, 1987.

[9] H. W. Horn, W. C. Swope, J. W. Pitera, J. D. Madura, T. J. Dick, G. L. Hura, and T. Head-Gordon, "Development of an improved four-site water model for biomolecular simulations: Tip4p-ew," *The Journal of Chemical Physics*, vol. 120, no. 20, pp. 9665–9678, 2004.

[10] J. Abascal, E. Sanz, R. García Fernández, and C. Vega, "A potential model for the study of ices and amorphous water: Tip4p/ice," *The Journal of Chemical Physics*, vol. 122, no. 23, 2005.

[11] J. L. Abascal and C. Vega, "A general purpose model for the condensed phases of water: Tip4p/2005," *The Journal of Chemical Physics*, vol. 123, no. 23, 2005.

[12] S. Izadi, R. Anandakrishnan, and A. V. Onufriev, "Building water models: a different approach," *The Journal of Physical Chemistry Letters*, vol. 5, no. 21, pp. 3863–3871, 2014.

[13] S. Piana, A. G. Donchev, P. Robustelli, and D. E. Shaw, "Water dispersion interactions strongly influence simulated structural properties of disordered protein states," *The Journal of Physical Chemistry B*, vol. 119, no. 16, pp. 5113–5123, 2015.

[14] M. A. González and J. L. Abascal, "A flexible model for water based on tip4p/2005," *The Journal of Chemical Physics*, vol. 135, no. 22, 2011.

[15] S. Habershon, T. E. Markland, and D. E. Manolopoulos, "Competing quantum effects in the dynamics of a flexible water model," *The Journal of Chemical Physics*, vol. 131, no. 2, 2009.

[16] F. H. Stillinger and A. Rahman, "Improved simulation of liquid water by molecular dynamics," *The Journal of Chemical Physics*, vol. 60, no. 4, pp. 1545–1557, 1974.

[17] M. W. Mahoney and W. L. Jorgensen, "A five-site model for liquid water and the reproduction of the density anomaly by rigid, nonpolarizable potential functions," *The Journal of Chemical Physics*, vol. 112, no. 20, pp. 8910–8922, 2000.

[18] S. W. Rick, "A reoptimization of the five-site water po-

tential (tip5p) for use with ewald sums," *The Journal of Chemical Physics*, vol. 120, no. 13, pp. 6085–6093, 2004.

[19] H. Nada, "Anisotropy in geometrically rough structure of ice prismatic plane interface during growth: Development of a modified six-site model of h2o and a molecular dynamics simulation," *The Journal of Chemical Physics*, vol. 145, no. 24, 2016.

[20] S. Izadi and A. V. Onufriev, "Accuracy limit of rigid 3-point water models," *The Journal of Chemical Physics*, vol. 145, no. 7, 2016.

[21] L.-P. Wang, T. J. Martinez, and V. S. Pande, "Building force fields: An automatic, systematic, and reproducible approach," *The Journal of Physical Chemistry Letters*, vol. 5, no. 11, pp. 1885–1891, 2014.

[22] R. Fuentes-Azcatl and J. Alejandre, "Non-polarizable force field of water based on the dielectric constant: Tip4p/ε," *The Journal of Physical Chemistry B*, vol. 118, no. 5, pp. 1263–1272, 2014.

[23] P. T. Kiss and A. Baranyai, "A systematic development of a polarizable potential of water," *The Journal of Chemical Physics*, vol. 138, no. 20, 2013.

[24] J. Reimers, R. Watts, and M. Klein, "Intermolecular potential functions and the properties of water," *Chemical Physics*, vol. 64, no. 1, pp. 95–114, 1982.

[25] C. Tainter, P. A. Pieniazek, Y.-S. Lin, and J. L. Skinner, "Robust three-body water simulation model," *The Journal of Chemical Physics*, vol. 134, no. 18, 2011.

[26] H. Yu, T. Hansson, and W. F. van Gunsteren, "Development of a simple, self-consistent polarizable model for liquid water," *The Journal of Chemical Physics*, vol. 118, no. 1, pp. 221–234, 2003.

[27] G. S. Fanourgakis and S. S. Xantheas, "The flexible, polarizable, thole-type interaction potential for water (ttm2-f) revisited," *The Journal of Physical Chemistry A*, vol. 110, no. 11, pp. 4100–4106, 2006.

[28] H. Jiang, O. A. Moultos, I. G. Economou, and A. Z. Panagiotopoulos, "Hydrogen-bonding polarizable intermolecular potential model for water," *The Journal of Physical Chemistry B*, vol. 120, no. 48, pp. 12358–12370, 2016.

[29] E. R. Pinnick, S. Erramilli, and F. Wang, "Predicting the melting temperature of ice-ih with only electronic structure information as input," *The Journal of Chemical Physics*, vol. 137, no. 1, 2012.

[30] K. Laasonen, F. Csajka, and M. Parrinello, "Water dimer properties in the gradient-corrected density functional theory," *Chemical Physics Letters*, vol. 194, no. 3, pp. 172–174, 1992.

[31] K. Laasonen, M. Sprik, M. Parrinello, and R. Car, ""ab initio"liquid water," *The Journal of Chemical Physics*, vol. 99, no. 11, pp. 9080–9089, 1993.

[32] M. Sprik, J. Hutter, and M. Parrinello, "Ab initio molecular dynamics simulation of liquid water: Comparison of three gradient-corrected density functionals," *The Journal of Chemical Physics*, vol. 105, no. 3, pp. 1142–1152, 1996.

[33] S. S. Xantheas, "Ab initio studies of cyclic water clusters (h2o) n, n= 1–6. iii. comparison of density functional with mp2 results," *The Journal of Chemical Physics*, vol. 102, no. 11, pp. 4505–4517, 1995.

[34] J. C. Grossman, E. Schwegler, E. W. Draeger, F. Gygi, and G. Galli, "Towards an assessment of the accuracy of density functional theory for first principles simulations of water," *The Journal of Chemical Physics*, vol. 120, no. 1, pp. 300–311, 2004.

[35] M. Chen, H.-Y. Ko, R. C. Remsing, M. F. Calegari Andrade, B. Santra, Z. Sun, A. Selloni, R. Car, M. L. Klein, J. P. Perdew, *et al.*, "Ab initio theory and modeling of water," *Proceedings of the National Academy of Sciences*, vol. 114, no. 41, pp. 10846–10851, 2017.

[36] L. Ruiz Pestana, O. Marsalek, T. E. Markland, and T. Head-Gordon, "The quest for accurate liquid water properties from first principles," *The Journal of Physical Chemistry Letters*, vol. 9, no. 17, pp. 5009–5016, 2018.

[37] M. J. Gillan, D. Alfe, and A. Michaelides, "Perspective: How good is DFT for water?," *The Journal of Chemical Physics*, vol. 144, no. 13, 2016.

[38] A. P. Gaiduk, F. Gygi, and G. Galli, "Density and compressibility of liquid water and ice from first-principles simulations with hybrid functionals," *The Journal of Physical Chemistry Letters*, vol. 6, no. 15, pp. 2902–2908, 2015.

[39] J. Schmidt, J. VandeVondele, I.-F. W. Kuo, D. Sebastiani, J. I. Siepmann, J. Hutter, and C. J. Mundy, "Isobaric- isothermal molecular dynamics simulations utilizing density functional theory: an assessment of the structure and density of water at near-ambient conditions," *The Journal of Physical Chemistry B*, vol. 113, no. 35, pp. 11959–11964, 2009.

[40] J. Wang, G. Román-Pérez, J. M. Soler, E. Artacho, and M.-V. Fernández-Serra, "Density, structure, and dynamics of water: The effect of van der waals interactions," *The Journal of Chemical Physics*, vol. 134, no. 2, 2011.

[41] G. Miceli, S. de Gironcoli, and A. Pasquarello, "Isobaric first-principles molecular dynamics of liquid water with nonlocal van der waals interactions," *The Journal of Chemical Physics*, vol. 142, no. 3, 2015.

[42] M. Ceriotti, J. Cuny, M. Parrinello, and D. E. Manolopoulos, "Nuclear quantum effects and hydrogen bond fluctuations in water," *Proceedings of the National Academy of Sciences*, vol. 110, no. 39, pp. 15591–15596, 2013.

[43] M. D. Baer, C. J. Mundy, M. J. McGrath, I.-F. W. Kuo, J. I. Siepmann, and D. J. Tobias, "Re-examining the properties of the aqueous vapor–liquid interface using dispersion corrected density functional theory," *The Journal of Chemical Physics*, vol. 135, no. 12, 2011.

[44] I.-C. Lin, A. P. Seitsonen, I. Tavernelli, and U. Rothlisberger, "Structure and dynamics of liquid water from ab initio molecular dynamics: Comparison of blyp, pbe, and revpbe density functionals with and without van der waals corrections," *Journal of Chemical Theory and Computation*, vol. 8, no. 10, pp. 3902–3910, 2012.

[45] J. VandeVondele, F. Mohamed, M. Krack, J. Hutter, M. Sprik, and M. Parrinello, "The influence of temperature and density functional models in ab initio molecular dynamics simulation of liquid water," *The Journal of Chemical Physics*, vol. 122, no. 1, 2005.

[46] L. Zheng, M. Chen, Z. Sun, H.-Y. Ko, B. Santra, P. Dhuvad, and X. Wu, "Structural, electronic, and dynamical properties of liquid water by ab initio molecular dynamics based on scan functional within the canonical ensemble," *The Journal of Chemical Physics*, vol. 148, no. 16, 2018.

[47] A. Zen, Y. Luo, G. Mazzola, L. Guidoni, and S. Sorella, "Ab initio molecular dynamics simulation of liquid water by quantum monte carlo," *The Journal of Chemical Physics*, vol. 142, no. 14, 2015.

[48] J. Behler and M. Parrinello, "Generalized neural-network

representation of high-dimensional potential-energy surfaces," *Physical Review Letters*, vol. 98, no. 14, p. 146401, 2007.

[49] T. Morawietz, V. Sharma, and J. Behler, "A neural network potential-energy surface for the water dimer based on environment-dependent atomic energies and charges," *The Journal of Chemical Physics*, vol. 136, no. 6, 2012.

[50] T. Morawietz, A. Singraber, C. Dellago, and J. Behler, "How van der waals interactions determine the unique properties of water," *Proceedings of the National Academy of Sciences*, vol. 113, no. 30, pp. 8368–8373, 2016.

[51] A. Singraber, T. Morawietz, J. Behler, and C. Dellago, "Density anomaly of water at negative pressures from first principles," *Journal of Physics: Condensed Matter*, vol. 30, no. 25, p. 254005, 2018.

[52] P. Montero de Hijes, S. Romano, A. Gorfer, and C. Dellago, "The kinetics of the ice–water interface from ab initio machine learning simulations," *The Journal of Chemical Physics*, vol. 158, no. 20, 2023.

[53] B. Cheng, J. Behler, and M. Ceriotti, "Nuclear quantum effects in water at the triple point: Using theory as a link between experiments," *The Journal of Physical Chemistry Letters*, vol. 7, no. 12, pp. 2210–2215, 2016.

[54] V. Kapil, J. Behler, and M. Ceriotti, "High order path integrals made easy," *The Journal of Chemical Physics*, vol. 145, no. 23, 2016.

[55] V. Kapil, D. M. Wilkins, J. Lan, and M. Ceriotti, "Inexpensive modeling of quantum dynamics using path integral generalized langevin equation thermostats," *The Journal of Chemical Physics*, vol. 152, no. 12, 2020.

[56] B. Cheng, E. A. Engel, J. Behler, C. Dellago, and M. Ceriotti, "Ab initio thermodynamics of liquid and solid water," *Proceedings of the National Academy of Sciences*, vol. 116, no. 4, pp. 1110–1115, 2019.

[57] T. Morawietz, O. Marsalek, S. R. Pattenaude, L. M. Streacker, D. Ben-Amotz, and T. E. Markland, "The interplay of structure and dynamics in the raman spectrum of liquid water over the full frequency and temperature range," *The Journal of Physical Chemistry Letters*, vol. 9, no. 4, pp. 851–857, 2018.

[58] A. Reinhardt and B. Cheng, "Quantum-mechanical exploration of the phase diagram of water," *Nature Communications*, vol. 12, no. 1, p. 588, 2021.

[59] B. Cheng, M. Bethkenhagen, C. J. Pickard, and S. Hamel, "Phase behaviours of superionic water at planetary conditions," *Nature Physics*, vol. 17, no. 11, pp. 1228–1232, 2021.

[60] O. Wohlfahrt, C. Dellago, and M. Sega, "Ab initio structure and thermodynamics of the rpbe-d3 water/vapor interface by neural-network molecular dynamics," *The Journal of Chemical Physics*, vol. 153, no. 14, 2020.

[61] A. Omranpour, P. Montero De Hijes, J. Behler, and C. Dellago, "Perspective: Atomistic simulations of water and aqueous systems with machine learning potentials," *The Journal of Chemical Physics*, vol. 160, no. 17, 2024.

[62] P. Montero de Hijes, C. Dellago, R. Jinnouchi, B. Schmiedmayer, and G. Kresse, "Comparing machine learning potentials for water: Kernel-based regression and behler–parrinello neural networks," *The Journal of Chemical Physics*, vol. 160, no. 11, 2024.

[63] G. Kresse and J. Furthmüller, "Efficient iterative schemes for ab initio total-energy calculations using a plane-wave basis set," *Physical review B*, vol. 54, no. 16, p. 11169, 1996.

[64] G. Kresse and J. Furthmüller, "Efficiency of ab-initio total energy calculations for metals and semiconductors using a plane-wave basis set," *Computational materials science*, vol. 6, no. 1, pp. 15–50, 1996.

[65] R. Jinnouchi, J. Lahnsteiner, F. Karsai, G. Kresse, and M. Bokdam, "Phase transitions of hybrid perovskites simulated by machine-learning force fields trained on the fly with bayesian inference," *Physical Review Letters*, vol. 122, no. 22, p. 225701, 2019.

[66] R. Jinnouchi, F. Karsai, and G. Kresse, "On-the-fly machine learning force field generation: Application to melting points," *Physical Review B*, vol. 100, no. 1, p. 014105, 2019.

[67] R. Jinnouchi, F. Karsai, C. Verdi, R. Asahi, and G. Kresse, "Descriptors representing two-and three-body atomic distributions and their effects on the accuracy of machine-learned inter-atomic potentials," *The Journal of Chemical Physics*, vol. 152, no. 23, 2020.

[68] C. Verdi, F. Karsai, P. Liu, R. Jinnouchi, and G. Kresse, "Thermal transport and phase transitions of zirconia by on-the-fly machine-learned interatomic potentials," *npj Computational Materials*, vol. 7, no. 1, p. 156, 2021.

[69] P. Liu, C. Verdi, F. Karsai, and G. Kresse, "α- β phase transition of zirconium predicted by on-the-fly machine-learned force field," *Physical Review Materials*, vol. 5, no. 5, p. 053804, 2021.

[70] B. Hammer, L. B. Hansen, and J. K. Nørskov, "Improved adsorption energetics within density-functional theory using revised perdew-burke-ernzerhof functionals," *Physical review B*, vol. 59, no. 11, p. 7413, 1999.

[71] S. Grimme, J. Antony, S. Ehrlich, and H. Krieg, "A consistent and accurate ab initio parametrization of density functional dispersion correction (dft-d) for the 94 elements h-pu," *The Journal of Chemical Physics*, vol. 132, no. 15, 2010.

[72] S. Grimme, S. Ehrlich, and L. Goerigk, "Effect of the damping function in dispersion corrected density functional theory," *Journal of computational chemistry*, vol. 32, no. 7, pp. 1456–1465, 2011.

[73] Y. Zhang and W. Yang, "Comment on "generalized gradient approximation made simple"," *Physical Review Letters*, vol. 80, no. 4, p. 890, 1998.

[74] J. Klimeš, D. R. Bowler, and A. Michaelides, "Chemical accuracy for the van der waals density functional," *Journal of Physics: Condensed Matter*, vol. 22, no. 2, p. 022201, 2009.

[75] J. Sun, A. Ruzsinszky, and J. P. Perdew, "Strongly constrained and appropriately normed semilocal density functional," *Physical review letters*, vol. 115, no. 3, p. 036402, 2015.

[76] L. Goerigk and S. Grimme, "A thorough benchmark of density functional methods for general main group thermochemistry, kinetics, and noncovalent interactions," *Physical Chemistry Chemical Physics*, vol. 13, no. 14, pp. 6670–6688, 2011.

[77] V. Holten, C. Bertrand, M. Anisimov, and J. Sengers, "Thermodynamics of supercooled water," *The Journal of Chemical Physics*, vol. 136, no. 9, 2012.

[78] D. Hare and C. Sorensen, "The density of supercooled water. ii. bulk samples cooled to the homogeneous nucleation limit," *The Journal of Chemical Physics*, vol. 87, no. 8, pp. 4840–4845, 1987.

[79] D. R. Lide, *CRC handbook of chemistry and physics*,

vol. 85. CRC press, 2004.

[80] T. Sotani, J. Arabas, H. Kubota, M. Kijima, and S. Asada, "Volumetric behaviour of water under high pressure at subzero temperature," *High Temperatures High Pressures*, vol. 32, no. 4, pp. 433–440, 2000.

[81] A. Eltareb, G. E. Lopez, and N. Giovambattista, "A continuum of amorphous ices between low-density and high-density amorphous ice," *Communications Chemistry*, vol. 7, no. 1, p. 36, 2024.

[82] J. Wong, D. A. Jahn, and N. Giovambattista, "Pressure-induced transformations in glassy water: A computer simulation study using the tip4p/2005 model," *The Journal of Chemical Physics*, vol. 143, no. 7, 2015.

[83] R. Khusnutdinoff, "Structural and dynamic features of water and amorphous ice," *Colloid Journal*, vol. 79, pp. 152–159, 2017.

[84] A. D. Fortes, "Accurate and precise lattice parameters of h2o and d2o ice ih between 1.6 and 270 k from high-resolution time-of-flight neutron powder diffraction data," *Acta Crystallographica Section B: Structural Science, Crystal Engineering and Materials*, vol. 74, no. 2, pp. 196–216, 2018.